Macromolecules

pubs.acs.org/Macromolecules Article

Skin-Inspired Healable Conductive Elastomers with Exceptional Strain-Adaptive Stiffening and Damage Tolerance

Xiaohan Wang, Yong-lei Wang, Xiao Yang, Zhongyuan Lu, Yongfeng Men, and Junqi Sun*

Cite This: *Macromolecules* 2021, 54, 10767−10775 Read Online

ACCESS | Metrics & More | Article Recommendations | Supporting Information

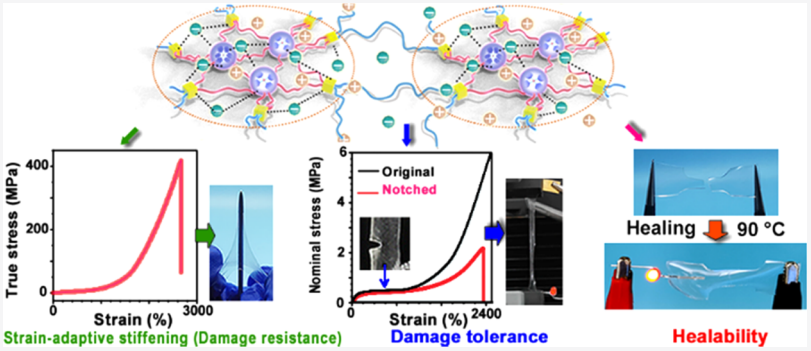

ABSTRACT: Stretchable conductive elastomers play an irreplaceable role in flexible electronic devices. However, stretchable conductive elastomers are usually soft and susceptible to damage. In this study, inspired from skin, highly stretchable and elastic conductive elastomers integrated with damage resistance, damage tolerance, and healability are fabricated by loading ionic liquids (ILs) within the polyurethane (PU) elastomers of the multiblock polymers of poly(dimethylsiloxane) (PDMS)/polycaprolactone (PCL) coordinated with Zn^{2+} ions. The mechanically robust conductive elastomer, with a tensile strength of ∼15.2 MPa and a stretchability of ∼2668%, has a satisfactory ionic conductivity of 2.9×10^{-4} S cm^{-1}. The conductive elastomer exhibits exceptional strain-adaptive stiffening, with an ∼100-fold increase in modulus when being fully stretched. The strain-adaptive stiffening endows the elastomer with excellent damage resistance. Meanwhile, the conductive elastomer has a record-high fracture energy of ∼33.8 kJ m^{-2}. The notched conductive elastomer can prevent the propagation of the notch up to a strain of ∼2400%. The exceptional strain-adaptive stiffening and damage tolerance originate from the *in situ* formed phase-separated domains, which are deformable and disintegrable under an external force to significantly strengthen the elastomer and dissipate energy. Furthermore, the conductive elastomer can be conveniently healed under heating to restore its original conductivity and mechanical properties.

1. INTRODUCTION

Conductive elastomers, which can autonomously recover their original shape as well as their electrical and/or ionic conductivity after stress release,[1−5] have attracted increasing attention from the scientific community because of their applicability as stretchable electrodes and wires in soft robotics, wearable intelligent devices, implantable electronics, and flexible displays.[3,4,6−10] However, conductive elastomers with enhanced stretchability are usually soft and susceptible to damage and fatigue, which results in functional deterioration and the electrical failure of the elastomer-based devices.[4,5,11−13] It is essential to fabricate conductive elastomers with enhanced reliability and durability. Such conductive elastomers are particularly required for soft and flexible devices operated under harsh conditions.[11,12,14] To achieve this, several properties should be integrated into conductive elastomers. One of the most crucial properties is damage resistance, which prevents the occurrence of damage and allows for the retention of the original structural integrity and conductivity of the devices when the conductive elastomers suffer from an external attack.[2,4] Second, the conductive elastomers should have the ability to prevent the propagation of damage once it occurs, which is termed damage tolerance.[8,15−17] With damage tolerance, the damaged conductive elastomers can retain most of their functions for continuous usage.[8,15−18] Third, the ability to fully heal damage is essential for conductive elastomers pursuing long service life.[4,5,13,14] Conductive elastomers exhibiting efficient healability can restore their original mechanical properties and conductivity either autonomously or with the assistance of an external stimulus.[4,5,8,11−14,18,19] Damage resistance, damage tolerance,

Received: September 20, 2021
Revised: October 25, 2021
Published: November 15, 2021

https://doi.org/10.1021/acs.macromol.1c01976
Macromolecules 2021, 54, 10767−10775

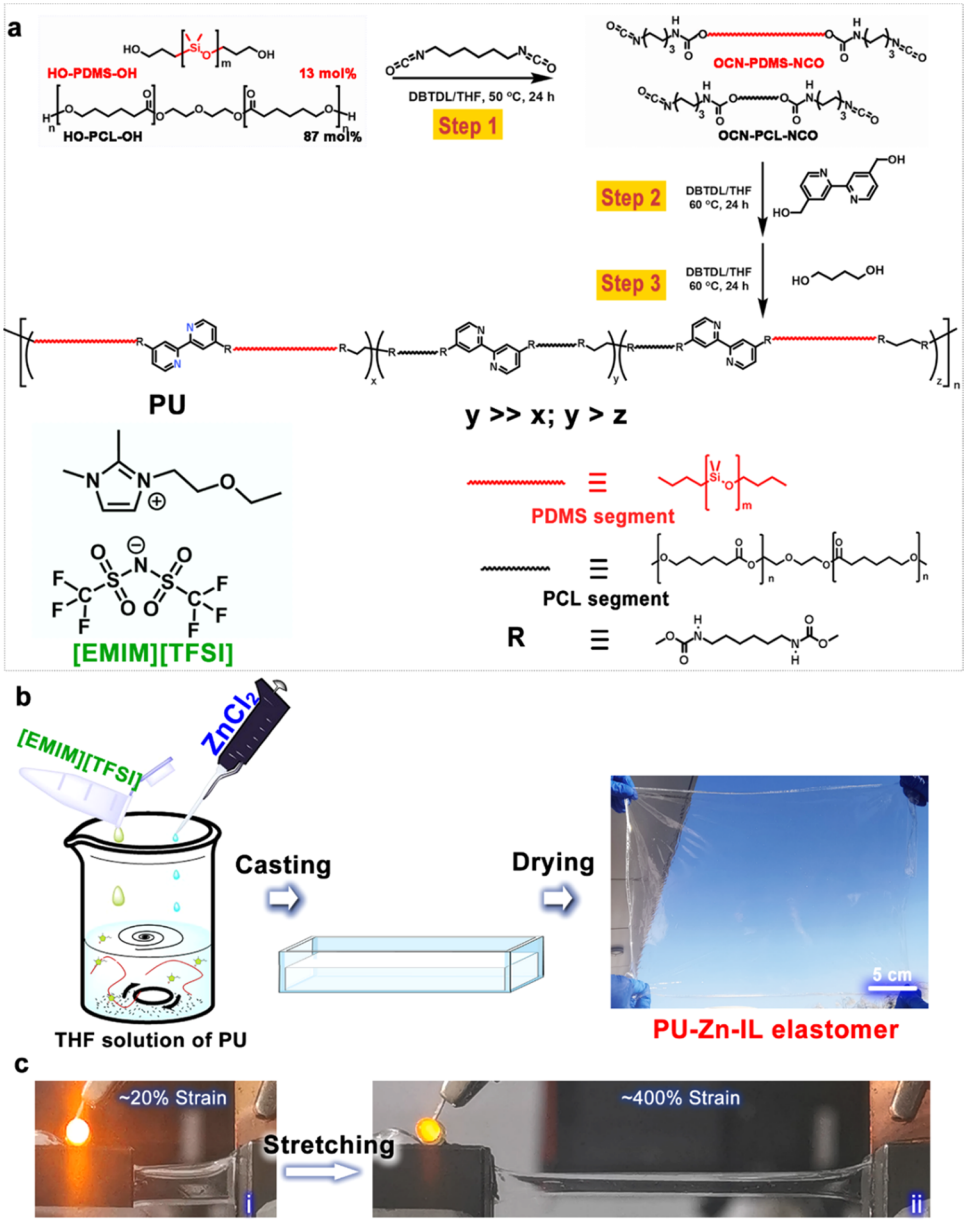

Figure 1. Fabrication process of the conductive elastomer. (a) Synthesis process of PU and the molecular structure of the loaded [EMIM][TFSI]. (b) Schematic illustration of the fabrication of the PU−Zn−IL elastomer. The digital image in (b) shows a piece of the PU−Zn−IL elastomer. (c) Digital images of the PU−Zn−IL elastomer at (i) ∼20% strain and (ii) ∼400% strain connected in a circuit with an LED bulb.

and healability provide a synergetic way to efficiently enhance the reliability and durability of conductive elastomers. Moreover, extensibility and resilience should also be further enhanced for conductive elastomers since these properties define the working range and fatigue resistance of the elastomers.[20]

To develop conductive elastomers with enhanced reliability and durability, several studies have focused on endowing conductive elastomers with healability and damage tolerance.[5,8,13,18] Conductive elastomers with healability have been fabricated by introducing dynamic interactions into their networks.[8,12−15] These conductive elastomers can restore their original structural integrity and conductivity by reconstructing the dynamically cross-linked networks in the damaged regions.[8,12−15] Healable and damage-tolerant conductive elastomers have also been fabricated by introducing dynamically cross-linked energy-dissipating structures within the healable elastomers.[8,21−23] The dissociation of sacrificial structures in the elastomers dissipates the energy concentrated in the damaged regions and prevents damage on the elastomer from further propagating.[8,17,21−23] Based on this design principle, a few types of healable conductive elastomers with damage tolerance were fabricated by embedding metal liquids within or by depositing metal films onto healable and damage-tolerant elastomers.[8,13,15,17,18] For instance, by depositing gold films onto hydrogen-bond-cross-linked polyurethanes with a tensile strength of ∼0.91 MPa and a fracture energy of ∼30 kJ m^{-2}, Chen and co-workers fabricated stretchable, damage-tolerant, and healable conductive elastomeric electrodes.[13] Without healing the mechanical damage, the stretched conductive elastomeric electrode can maintain satisfactory conductivity at a strain <40% without further tearing the elastomer.[13,15,17] Healable conductive elastomers with damage tolerance demonstrate largely enhanced reliability and

https://doi.org/10.1021/acs.macromol.1c01976
Macromolecules 2021, 54, 10767−10775

durability compared with conductive elastomers with only healability.[4,5,11,14,24] However, conductive elastomers simultaneously integrated with damage resistance, damage tolerance, and healability have never been reported.

Natural skin is initially soft to accommodate the movement of the body but stiffens rapidly to increase its strength by several orders of magnitude once it is considerably stretched.[2,25−27] This nonlinear mechanical phenomenon of skin is known as strain-adaptive stiffening, which endows natural skin with excellent damage resistance and helps the skin to actively avoid injury when subjected to attack.[2,25] When an injury occurs, the natural skin can prevent the injury from further propagation and subsequently autonomously heal the injury.[4,26,27] Inspired by the functions of natural skin, we herein report the fabrication of mechanically robust, highly stretchable, and elastic conductive elastomers with damage resistance, damage tolerance, and healability. The conductive elastomers, with an ionic conductivity of 2.9×10^{-4} S cm^{-1}, are fabricated by loading ionic liquids (ILs) within polyurethane (PU) elastomers of multiblock polymers of poly(dimethylsiloxane) (PDMS)/polycaprolactone (PCL) coordinated with Zn^{2+} ions. The *in situ* formed dynamic hierarchical domains, which contain coordination and hydrogen bonds, ion−dipole forces, and PCL segments, are stable at low strains to ensure the excellent elasticity and resilience of the conductive elastomers. When the conductive elastomers are considerably stretched, the deformation and even the dissociation of the dynamic hierarchical domains can efficiently dissipate energy to endow the elastomers with excellent extensibility, strain-adaptive stiffening (*i.e.*, damage resistance), and damage tolerance. Because of the reversibility of the hydrogen and coordination bonds under heating, the conductive elastomers can be efficiently healed to restore their original mechanical performance and conductivity.

2. EXPERIMENTAL SECTION

2.1. Materials. Polycaprolactone diol (HO−PCL−OH, M_n = 2000 Da) and bis(hydroxyalkyl)-terminated poly(dimethylsiloxane) (HO−PDMS−OH, M_n = 5600 Da) were obtained from Sigma-Aldrich. Hexamethylene diisocyanate (HMDI), butanediol (BDO), and di-*n*-butyltin dilaurate (DBTDL) were purchased from Tokyo Chemical Industry Co., Ltd. [2,2′-Bipyridine]-4,4′-dimethanol (HO−BPY−OH), dried tetrahydrofuran (THF), and hexane were purchased from Changchun Sanbang Pharmaceutical Technology Co., Ltd. 1-Ethoxyethyl-3-methylimidazolium bis(trifluoromethanesulfonyl)imide ([EMIM][TFSI]) was obtained from Lanzhou Institute of Chemical Physics.

2.2. Synthesis of the Prepolymers. HO−PCL−OH (14.00 g, 7.00 mmol) and HO−PDMS−OH (6.00 g, 1.07 mmol) were dissolved in dried THF (200 mL) under continuous stirring. HMDI (2.74 g, 16.14 mmol) and di-*n*-butyltin dilaurate (0.10 g, 0.16 mmol) were then added to the above THF solution. This solution was continuously stirred at 60 °C in a N_2 atmosphere for 24 h to obtain the prepolymer solution.

2.3. Synthesis of Polyurethane (PU). For the synthesis of PU, HO−BPY−OH (1.30 g, 6.06 mmol) was added into the prepolymer solution (22.74 g, 8.08 mmol), which was stirred at 60 °C for 24 h in a N_2 atmosphere. Subsequently, BDO (0.18 g, 2.02 mmol) was charged into the above solution. The resulting solution was heated to 60 °C and continuously stirred in a N_2 atmosphere for 24 h. The reaction solution was poured into hexane (2000 mL) to precipitate the PU. The precipitate was collected and dried under vacuum for 24 h to obtain PU (19.8 g, 93.3%).

2.4. Fabrication of PU−Zn−IL Elastomers. A THF solution of $ZnCl_2$ (0.7 mol L^{-1}) with a molar ratio of Zn^{2+} ions to bipyridine groups in PU being 2:3 was added to a THF solution of PU (5 g L^{-1}). After stirring for 4 h at room temperature, [EMIM][TFSI] with the same mass of PU was added into the above THF solution, which was further stirred for another 4 h. The resultant organogel was then cast onto a piece of a cleaned glass plate. After evaporation of THF, PU−Zn−IL elastomer was obtained by peeling off the elastomer from the glass plate.

3. RESULTS AND DISCUSSION

3.1. Fabrication of Conductive Elastomers. The conductive elastomers were fabricated by loading the ionic liquids (ILs) of [EMIM][TFSI] within PU elastomers. The PU elastomers are multiblock polymers of PDMS and PCL cross-linked with hydrogen bonds and coordination bonds between the bipyridine groups and Zn^{2+} ions.[21] The synthesis of PU is schematically shown in Figure 1a. Briefly, isocyanate-terminated PDMS and PCL prepolymers were first synthesized through the reaction of HMDI with a mixture of HO−PCL−OH and HO−PDMS−OH. Then, HO−BPY−OH and BDO as chain extenders were sequentially added to the reaction system to obtain PU. The feed molar ratio of HMDI, HO−PCL−OH, HO−PDMS−OH, HO−BPY−OH, and BDO was 2:0.87:0.13:0.75:0.25. According to the gel permeation chromatography (GPC) results, the number-average molecular weight (M_n) of PU was calculated as 74 kDa with a polydispersity index (PDI) of 1.28 (Figure S1, Supporting Information). As indicated in Figure 1b, the conductive elastomers were fabricated by cross-linking PU with Zn^{2+} ions and loading ILs into Zn^{2+} cross-linked PU (PU−Zn). THF solutions of $ZnCl_2$ and ILs were sequentially added into the THF solution of PU under stirring. The conductive elastomer was obtained by casting the organogel of PU, Zn^{2+} ions, and ILs onto a glass plate followed by the evaporation of THF. The feed molar ratio of the Zn^{2+} ions to the bipyridine groups in PU was 2:3, and the mass ratio of the ILs to PU was 1:1. For simplicity, the conductive elastomer is denoted as the PU−Zn−IL elastomer. The digital image in Figure 1b indicates that the as-prepared sheet-like PU−Zn−IL elastomer with an area of 0.3 × 0.4 m^2 and a thickness of ∼0.2 mm is highly transparent and defect-free (Figure S2, Supporting Information). Thermogravimetric analysis (TGA) shows that the PU−Zn−IL conductive elastomer is thermally stable at temperatures lower than 238 °C (Figure S3, Supporting Information). The conductivity of the PU−Zn−IL elastomer is as high as 2.9×10^{-4} S cm^{-1} when measured at room temperature and ∼40% relative humidity (RH). In a highly humid environment with ∼100% RH, the PU−Zn−IL conducive elastomer has an increased conductivity of 4.2×10^{-3} S cm^{-1} because the water adsorbed in the elastomer can enhance the mobility of hydrophilic ILs. The light-emitting diode (LED) bulb connected by the PU−Zn−IL elastomer is thus lit due to good ionic conductivity of the elastomer (Figure 1c). Furthermore, the LED bulb remains lit when the PU−Zn−IL elastomer is stretched from a strain of 0 to 400% or even further, demonstrating that the conductive elastomer can maintain satisfactory conductivity in a highly stretched state (Figure 1c and Movie S1, Supporting Information). The brightness of the LED bulb decreases during the stretching process, indicating that the electric resistance (R) of the PU−Zn−IL elastomer increases as the strain increases (Figure 1c and Movie S1, Supporting Information). Fourier transform infrared (FT-IR) spectroscopy confirms that there exist coordination bonds between the bipyridine groups and Zn^{2+} ions in the PU−Zn−IL elastomers (Figure S4, Supporting

https://doi.org/10.1021/acs.macromol.1c01976
Macromolecules 2021, 54, 10767−10775

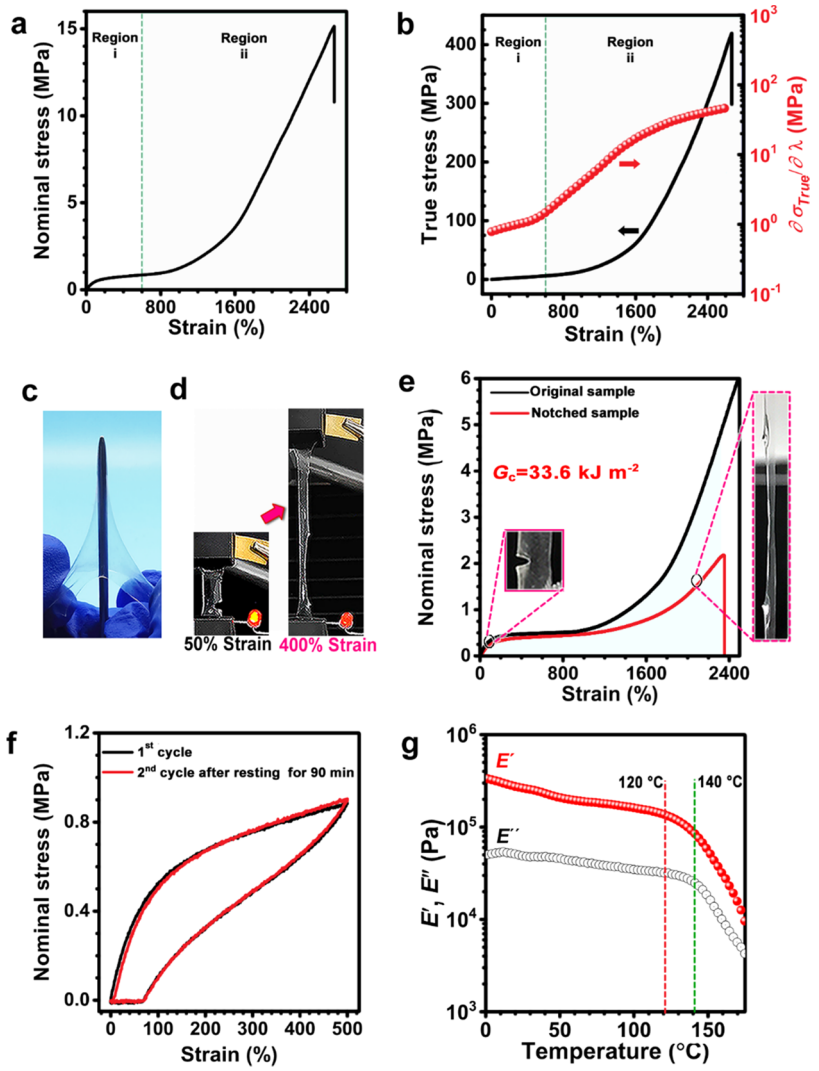

Figure 2. Mechanical properties of the PU−Zn−IL elastomer. (a) Typical nominal stress−strain curve of the PU−Zn−IL elastomer. (b) Typical true stress−strain and modulus−strain curves of the PU−Zn−IL elastomer. (c) Puncture demonstration of the PU−Zn−IL elastomer with a needle. (d) Digital images of the notched PU−Zn−IL elastomer at ∼50 and ∼200% strains. The original length, thickness, and width of the intact elastomer film are ∼10, ∼0.2, and ∼5 mm, respectively. The length of the notch is ∼2 mm. (e) Typical stress−strain curves of the intact and notched PU−Zn−IL elastomers. The inset images are magnified views of the notch at ∼50 and ∼2000% strains. (f) Loading−unloading curves of the PU−Zn−IL elastomer that were measured with an ∼90 min rest time between each cycle. (g) Storage moduli (E') and loss moduli (E'') of the PU−Zn−IL elastomer as a function of temperature.

Information). The density functional theory (DFT) calculations reveal that the Zn^{2+}-coordinated bipyridine complexes are bidentate chelates ($Zn[BPY]_2^{2+}$) or tridentate chelates ($Zn[BPY]_3^{2+}$) with binding energies of −111.67 and −112.58 kJ mol^{-1}, respectively (Table S1, Supporting Information). DFT calculations also show that the cis and trans TFSI anions form ion−dipole interactions with Zn^{2+}-coordinated bipyridine complexes, urethane groups, PDMS, and PCL segments. The binding energies of the ion−dipole interactions of the TFSI anions with $Zn[BPY]_2^{2+}$, $Zn[BPY]_3^{2+}$, and the urethane groups are around −250, −10, and −85 kJ mol^{-1}, respectively (Table S1, Supporting Information). The rheological curves of the THF solutions of PU−Zn before and after the addition of ILs were also measured (Figure S5, Supporting Information). The storage modulus (E') of the THF solution of PU−Zn is smaller than the loss modulus (E'') from 1 to 20 rad s^{-1}. After the addition of ILs, E' becomes higher than E'', indicating that a sol-to-gel transition had taken place.[28,29] This result confirms the stable interactions of the IL with the PU−Zn elastomers.

3.2. Mechanical Properties of PU−Zn−IL Elastomers.

The mechanical properties of the PU−Zn−IL elastomer were investigated by uniaxial tensile tests with a stretching speed of 50 mm min^{-1} at room temperature. The typical nominal stress−strain curve in Figure 2a shows that the PU−Zn−IL elastomer exhibits the mechanical property of a typical elastomer because no yielding phenomenon appears during elongation.[21] The PU−Zn−IL elastomer has a tensile strength, toughness, and strain at break of ∼15.2 MPa, ∼117.7 MJ m^{-3}, and ∼2668%, respectively. To the best of our knowledge, the comprehensive mechanical properties of the PU−Zn−IL conductive elastomers in terms of the tensile strength and strain at break are noticeably higher than those of previously reported IL-based conductive materials (Figure S6, Supporting Information).[4,8,16,24] It should be noted that the mechanical properties and conductivity of the conductive elastomers can

https://doi.org/10.1021/acs.macromol.1c01976
Macromolecules 2021, 54, 10767−10775

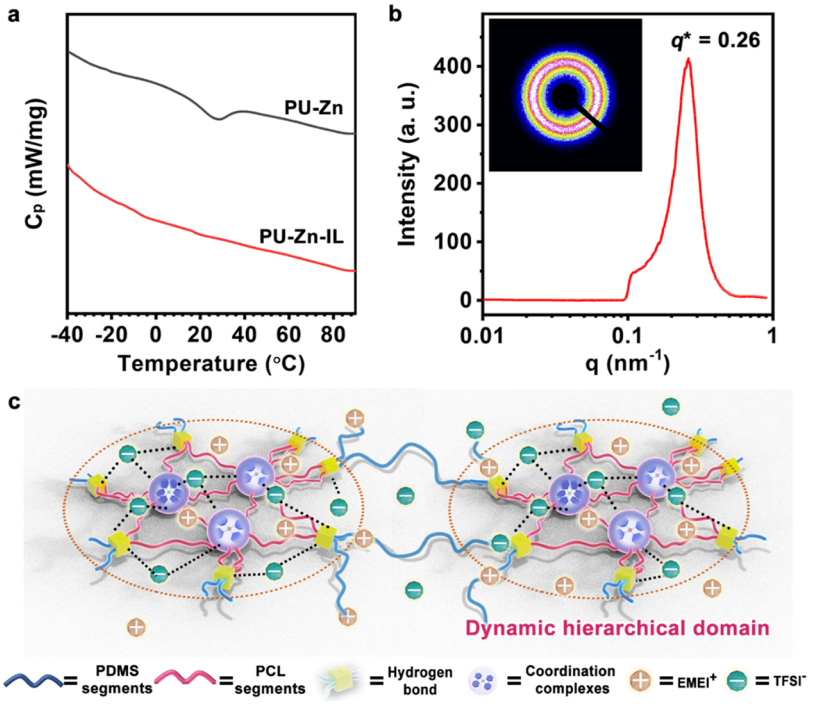

Figure 3. Structural characterization of the PU−Zn−IL elastomer. (a) DSC curves of the PU−Zn and PU−Zn−IL elastomers. (b) SAXS pattern of the PU−Zn−IL elastomer. The inset map is the 2D-SAXS patterns of the PU−Zn−IL elastomer. (c) Schematic illustration of the structure of the PU−Zn−IL elastomer.

be tailored by the mass ratio of loaded ILs to PU. The PU−Zn−IL conductive elastomers with a mass ratio of the ILs to PU being 1:1 have the optimized tensile strength and ionic conductivity (Figure S7, Supporting Information). The stress−strain curve of the PU−Zn−IL elastomer can be divided into two regions. When the strain is below 600%, the stress of the PU−Zn−IL elastomer increases steadily and slowly (Figure 2a, region i). However, when the strain is above 600%, the increase in stress becomes more pronounced (Figure 2a, region ii). To further evaluate this nonlinear mechanical character of the PU−Zn−IL elastomer, the curves of the true stress and the ∂true stress/∂strain (modulus) as a function of strains were obtained. As shown in Figure 2b, the true stress increases slowly and almost linearly from 0 to 8.6 MPa as the PU−Zn−IL elastomer is subjected to a strain from 0 to 600%. The true stress of the elastomer increases exponentially upon further stretching from 600% strain until breakage. Interestingly, the characteristic sigmoid shape of the modulus−strain curve is similar to that of skin.[4,25] As the PU−Zn−IL elastomer is stretched from 0 to 600% and then to the breaking strain, its modulus first steadily increases from 0.53 to 0.86 MPa and then rapidly increases to 49.9 MPa, which is almost 100 times higher than its original modulus. The nonlinear mechanical behavior of the PU−Zn−IL elastomer is similar to the strain-adaptive stiffening of natural skin, which stiffens rapidly during deformation.[4,25] Like natural skin, the PU−Zn−IL elastomer also exhibits good damage resistance. As shown in Figure 2c, the PU−Zn−IL elastomer with a thickness of ∼0.2 mm can withstand needle puncture.

Besides the strain-adaptive stiffening, the damage tolerance of the PU−Zn−IL elastomer was assessed by stretching the elastomer (∼5 mm in width and ∼10 mm in length) with an ∼2 mm notch on one side. The notched elastomer can be stretched to 400% strain with no propagation of the notch being observed. The connected LED bulb remains lit during elongation (Figure 2d, and Movie S2, Supporting Information). The fracture energy (G_c) of the PU−Zn−IL elastomer was measured following the method developed by Greensmith.[8,21,30] To do so, a notch with a length of ∼1 mm was introduced on one side of the PU−Zn−IL elastomer with a size of ∼5 mm in width, ∼10 mm in length, and ∼0.2 mm in thickness. The notched elastomer was stretched at a speed of 3 mm min^{-1} (Figure 2e, inset). The notched elastomer could be stretched to ∼2400% strain without propagation of the notch (Figure 2e). Its fracture energy was calculated to be 33.8 kJ m^{-2}, which is higher than any previously reported conductive elastomer in the literature (Figure S8, Supporting Information).[8,13,15] The cyclic stress−strain curves of the PU−Zn−IL elastomer were measured to evaluate its elasticity. As shown in Figure 2f, when being stretched to ∼500% strain and then released, the PU−Zn−IL elastomer exhibits a hysteresis loop with an area of 1.3 MJ m^{-3}. After resting at room temperature for 90 min, the second loading−unloading curve overlaps with the first one, demonstrating the excellent elasticity and resilience of the PU−Zn−IL elastomer. The temperature-dependent oscillation rheology curves in Figure 2g show that the E' of the PU−Zn−IL elastomer decreases relatively slowly and remains at a constant order of magnitude as the temperature increases from 0 to ∼120 °C, indicating the excellent thermomechanical stability of the PU−Zn−IL elastomer. When the temperature is above ∼140 °C, E' and E'' decrease rapidly, which means that a large fraction of the physical cross-linkers in the elastomer is broken.[31] However, the PU−Zn−IL elastomer remains in the solid state at temperatures <175 °C because its E' is still higher than its E''. Considering its high mechanical strength and its excellent extensibility, elasticity, and thermomechanical stability, the PU−Zn−IL elastomer is believed to be suitable for use in

https://doi.org/10.1021/acs.macromol.1c01976
Macromolecules 2021, 54, 10767−10775

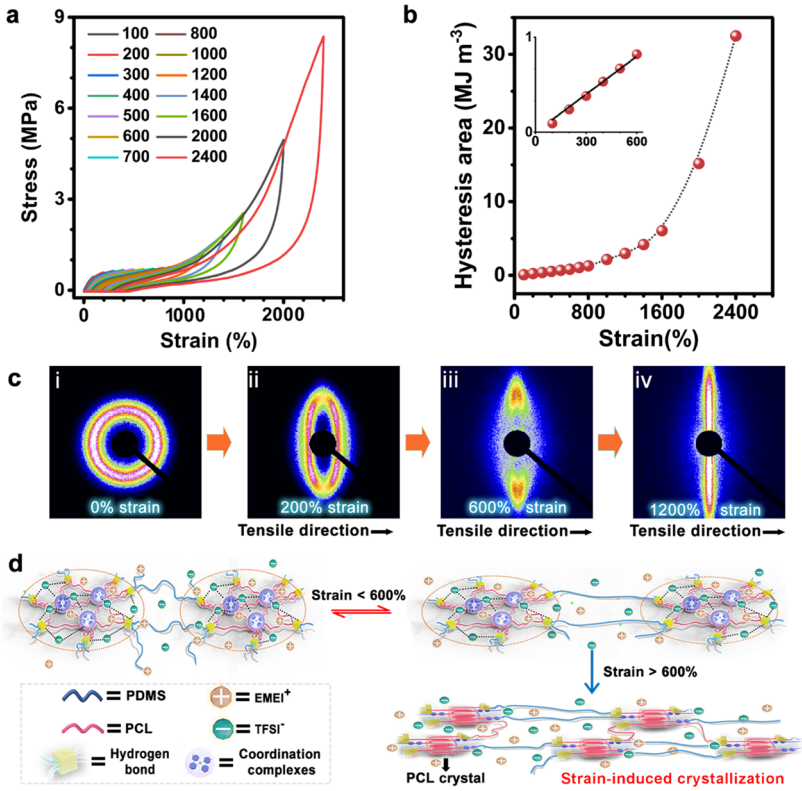

Figure 4. Mechanism of the strain-adaptive stiffening and damage tolerance of the PU−Zn−IL elastomer. (a) Typical cyclic stress−strain curve of the PU−Zn−IL elastomer. (b) Corresponding hysteresis area at each loading−unloading cycle. (c) 2D-SAXS patterns of the PU−Zn−IL elastomer at strains of 0% (i), 200% (ii), 600% (iii), and 1200% (iv). (d) Proposed mechanism of the strain-adaptive stiffening and damage tolerance of the PU−Zn−IL elastomer.

strain sensors, stretchable electrodes, and wires for a large variety of flexible devices. Figure S9 shows that the PU−Zn−IL conductive elastomer exhibits highly reversible and repeatable resistance changes under 0.5, 1, 5, and 10% strains, indicating its excellent strain sensing ability.[32,33]

3.3. Structure of the PU−Zn−IL Elastomer. The structure of the PU−Zn−IL elastomer was characterized with differential scanning calorimetry (DSC), wide-angle X-ray diffraction (WAXD), and small-angle X-ray scattering (SAXS). As shown in Figure 3a, the DSC curve of the PU−Zn elastomer shows an endothermic transition peak at around 35 °C, which is attributed to the melting of the PCL crystals.[21] By contrast, the DSC curve of the PU−Zn−IL elastomer does not show a detectable transition peak. The WAXD of the PU−Zn−IL elastomer exhibits two diffraction halos at 2θ = 12.4 and 20.2°, which have the calculated orientation order parameter (f) of 0.023 and 0.029, respectively (Figure S10, Supporting Information), indicating that PDMS and PCL segments are amorphous and homogeneously existed in the PU−Zn−IL elastomer.[21,34] These results indicate that in the PU−Zn−IL elastomer, the PCL crystals are dissolved by the loaded ILs. The two-dimensional SAXS (2D-SAXS) patterns of the PU−Zn−IL elastomer consist of concentric circles (inset map in Figure 3b), indicating that the aggregates of the electron-rich motifs are isotropically dispersed in the elastomer.[21,35−37] The electron-rich motifs in the PU−Zn−IL elastomer are Zn^{2+}-coordinated bipyridine complexes, urethane groups, and the bonded TFSI anions.[21,35,36] Considering that the number of PCL segments in the PU chains is larger than that of the PDMS segments, it is inferred that most bipyridine and urethane groups are interlocked within the PCL segments. Therefore, it is speculated that the electron-rich motifs are linked by amorphous PCL segments and co-form the aggregates (*i.e.*, phase-separated domains). The PDMS segments that act as the network strands are dynamically cross-linked by the *in situ* formed phase-separated domains to form a stable elastomer network (Figure 3c). The one-dimensional SAXS (1D-SAXS) patterns of the PU−Zn−IL elastomer derived from its 2D-SAXS patterns only show a strong principal scattering peak (q^*) at 0.26 nm^{-1} (Figure 2b). The structural periodicity (D) of the phase-separated domains calculated from the 1D-SAXS patterns is 24.2 nm ($D = 2\pi/q^*$).[36] Considering the high conductivity of the PU−Zn−IL elastomer, the ILs can also be dispersed within the PDMS segments of the PU−Zn−IL elastomer. Based on the above results and analysis, the structure of the PU−Zn−IL elastomer is schematically shown in Figure 3c.

3.4. Mechanism of Strain-Adaptive Stiffening and Damage Tolerance. With the aim to further characterize the strain-adaptive stiffening and damage tolerance, the energy dissipation of the PU−Zn−IL elastomer at different strains was characterized using a cyclic tensile test with an increasing strain but no delay time (Figure 4a). The hysteresis area, which corresponds to the dissipated energy during each loading−unloading cycle,[38] as a function of strain is plotted in Figure 4b. Upon stretching the PU−Zn−IL elastomer from a strain of 0 to 600%, its hysteresis area increases linearly but slowly, demonstrating that few interactions among the polymer chains are disassociated. This result indicates that the PU−Zn−IL elastomer mainly undergoes recoverable elastic deformation during this process. In contrast, as the strain further increases, the hysteresis area increases rapidly, meaning that obvious and

https://doi.org/10.1021/acs.macromol.1c01976
Macromolecules 2021, 54, 10767−10775

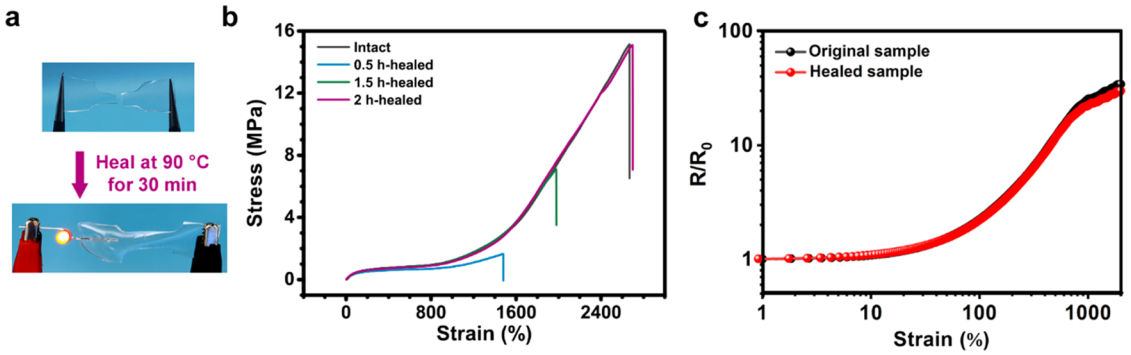

Figure 5. Healability of the PU−Zn−IL elastomer. (a) Digital images of the healing process of the PU−Zn−IL elastomer. (b) Typical stress−strain curves of the original and the fractured PU−Zn−IL elastomers healed for different lengths of time. (c) Relative resistance changes of the original and healed PU−Zn−IL elastomers as a function of strain.

irreversible structural changes (*i.e.*, disassociation of dynamic interactions among the polymer chains) take place during this stretching process. The structural changes in the stretched PU−Zn−IL elastomer were characterized *via* 2D-SAXS and WAXD. After stretching the PU−Zn−IL elastomer to 200% strain, the WAXD patterns of the elastomer do not show obvious changes compared with those of the intact elastomer, indicating that the PU−Zn−IL elastomer is still amorphous (Figure S10a, Supporting Information). Meanwhile, the scattering cycles of the PU−Zn−IL elastomer at 200% strain become elliptical in shape, showing that the electron-rich structures in the elastomer are oriented along the stretching direction but the phase-separated domains still maintain their structural integrity (Figure 4c-i,ii).[32,37] Upon stretching the PU−Zn−IL elastomer to 600% strain or further, new scattering signals perpendicular to the tensile direction were observed in the 2D-SAXS patterns (Figure 4c-iii,iv).[21,34,37] Meanwhile, a new diffraction peak at $2\theta = 21.5°$ appears in the WAXD patterns, which corresponds to the 110 plane of PCL crystals (Figure S10a, Supporting Information).[21,34] These results indicate that the phase-separated domains in the PU−Zn−IL elastomer are gradually disintegrated, accompanied by the strain-induced crystallization (SIC) of the PCL segments.[34,39,40]

The mechanism of the exceptional strain-adaptive stiffening and damage tolerance of the PU−Zn−IL elastomers is schematically illustrated in Figure 4d. The strain-adaptive stiffening undergoes two stages, *i.e.*, the extension of network strands (PDMS segments) and the disintegration of phase-separated domains. When the elastomers are stretched to small strains (<600%), the randomly coiled PDMS segments in the elastomer are preferentially uncoiled, whereas the phase-separated domains maintain their structural integrity. The modulus and strength of the PU−Zn−IL elastomer slowly increase. Upon further stretching the PU−Zn−IL elastomer (strains >600%), the PCL chains in the dynamic phase-separated domains begin to slip along the tensile direction, and the disassociation of the dynamic interactions occurs. Ultimately, the phase-separated domains are disintegrated. In this process, the PCL segments gradually align along the stretching direction to crystallize, and the hidden length in the hierarchical domains is released. The newly formed PCL crystals significantly increase the energy barrier for chain slipping.[23,41] Therefore, a continuously increasing force is required to further stretch the elastomer, causing a significant increase in stiffness.[23] As a result, the PU−Zn−IL elastomer exhibits skin-like strain-adaptive stiffening, which endows the elastomer with damage resistance. Moreover, the disintegration of the phase-separated domains, including the breakage of dynamic interactions and the slippage of PCL chains, can effectively dissipate applied energy concentrated on the damage regions, endowing the PU−Zn−IL elastomer excellent damage tolerance.[21,23]

3.5. Healability of the PU−Zn−IL Elastomer. The healability of the PU−Zn−IL elastomer was examined using fully cut elastomer sheets. As shown in Figure 5a, the separated PU−Zn−IL elastomers were brought into contact and then heated at 90 °C. After heating for 30 min, the cut on the re-connected elastomer completely disappeared. The LED bulb connected by the healed PU−Zn−IL elastomer is lit. In addition, the healability of the PU−Zn−IL elastomer is time-dependent, with the healing efficiency increasing with increasing heating time. After heating for 2 h, the stress−strain curve of the healed PU−Zn−IL elastomer almost overlaps with that of the pristine elastomer, indicating that the damage was fully healed (Figure 5b). During the healing process, the PU−Zn−IL elastomer can still maintain its original shape. Figure 5c shows the resistance changes (R/R_0) of the healed and pristine PU−Zn−IL elastomers as a function of their tensile strains. The overlap of these two curves further confirms that the PU−Zn−IL elastomer was fully healed. The healing mechanism of the PU−Zn−IL elastomer can be described as follows: When the fractured elastomers are heated at 90 °C, the coordination bonds, hydrogen bonds, and ion−dipole interactions in the PU−Zn−IL elastomer are dynamically broken. The mobility of the polymer chains at the fractured surfaces is largely enhanced.[23] The interdiffusion of the polymer chains in the fractured surfaces enables the reorganization of polymer chains in the damaged regions and the dynamic rebuilding of interactions among the polymer chains.[23,42,43] In this way, the fractured PU−Zn−IL elastomer is fully healed, and its original mechanical and conductive properties are restored. The rupture and reformation of the supramolecular interactions within the PU−Zn−IL elastomers during the healing process were further confirmed by strain relaxation experiments (Figure S11, Supporting Information).

4. CONCLUSIONS

In summary, we successfully fabricated transparent, mechanically robust, highly stretchable, and elastic PU−Zn−IL conductive elastomers integrated with excellent damage resistance, damage tolerance, and healability. The PU−Zn−

https://doi.org/10.1021/acs.macromol.1c01976
Macromolecules 2021, 54, 10767−10775

IL elastomer exhibits unique strain-adaptive stiffening (damage tolerance) and superior damage tolerance with a fracture energy of ~33.8 kJ m^{-2}. The exceptional damage resistance and tolerance of the PU−Zn−IL elastomer can be attributed to the *in situ* formed deformable and disintegrable phase-separated domains, which are aggregates of PCL segments, Zn^{2+}-coordinated bipyridine complexes, hydrogen-bonded urethane groups, and the loaded ILs. The phase-separated domains serve as a rigid nanofiller to strengthen the elastomer and enhance its elasticity. Moreover, the deformation and disintegration of the phase-separated domains endow the PU−Zn−IL elastomer with excellent strain-adaptive stiffening and high fracture energy. The damaged PU−Zn−IL elastomer also demonstrates highly efficient healability under heating. The synergy of the strain-adaptive stiffening, damage tolerance, and healability effectively enhances the reliability and durability of the PU−Zn−IL elastomers. This study opens new avenues for the fabrication of stretchable conductive elastomers and other types of soft materials with ultrahigh reliability and durability by simultaneously integrating with strain-adaptive stiffening, damage tolerance, and healability.

■ ASSOCIATED CONTENT

Supporting Information

The Supporting Information is available free of charge at https://pubs.acs.org/doi/10.1021/acs.macromol.1c01976.

DFT calculations, the method to obtain true stress−strain curves, the method to calculate fracture energy of the elastomers, characterizations, and supporting figures (PDF)

LED bulb connected by the PU−Zn−IL elastomer (Movie S1) (MP4)

Notched PU−Zn−IL elastomer can prohibit the propagation of notch during the stretching process (Movie S2) (MP4)

■ AUTHOR INFORMATION

Corresponding Author

Junqi Sun − *State Key Laboratory of Supramolecular Structure and Materials, College of Chemistry, Jilin University, Changchun 130012, P. R. China;* orcid.org/0000-0002-7284-9826; Email: sun_junqi@jlu.edu.cn

Authors

Xiaohan Wang − *State Key Laboratory of Supramolecular Structure and Materials, College of Chemistry, Jilin University, Changchun 130012, P. R. China*

Yong-lei Wang − *Department of Materials and Environmental Chemistry, Arrhenius Laboratory, Stockholm University, SE-106 91 Stockholm, Sweden;* orcid.org/0000-0003-3393-7257

Xiao Yang − *State Key Laboratory of Polymer Physics and Chemistry, Changchun Institute of Applied Chemistry, Chinese Academy of Sciences, Changchun 130022, P. R. China;* orcid.org/0000-0001-7488-1339

Zhongyuan Lu − *State Key Laboratory of Supramolecular Structure and Materials, College of Chemistry, Jilin University, Changchun 130012, P. R. China;* orcid.org/0000-0001-7884-0091

Yongfeng Men − *State Key Laboratory of Polymer Physics and Chemistry, Changchun Institute of Applied Chemistry, Chinese Academy of Sciences, Changchun 130022, P. R. China;* orcid.org/0000-0003-3277-2227

Complete contact information is available at: https://pubs.acs.org/10.1021/acs.macromol.1c01976

Notes

The authors declare no competing financial interest.

■ ACKNOWLEDGMENTS

This work was financially supported by National Natural Science Foundation of China (NSFC grant nos. 21935004 and 21774049) and China Postdoctoral Science Foundation (nos. BX20190138 and 2019M661201).

■ ABBREVIATIONS

ILs, ionic liquids; PU, polyurethane; PDMS, poly(dimethylsiloxane); PCL, polycaprolactone; [EMIM][TFSI], 1-ethoxyethyl-3-methylimidazolium bis(trifluoromethanesulfonyl)imide; HMDI, hexamethylene diisocyanate; HO−PCL−OH, PCL diol; HO−PDMS−OH, bis(hydroxyalkyl)-terminated PDMS; HO−BPY−OH, [2,2′-bipyridine]-4,4′-dimethanol; BDO, butanediol; GPC, gel permeation chromatography; M_n, number-average molecular weight; PDI, polydispersity index; THF, tetrahydrofuran; PU−Zn, Zn^{2+} cross-linked PU; TGA, thermogravimetric analysis; LED, light-emitting diode; *R*, electric resistance; FT-IR, Fourier transform infrared; DFT, density functional theory; *E*′, storage moduli; *E*″, loss moduli; G_c, fracture energy; DSC, differential scanning calorimetry; WAXD, wide-angle X-ray diffraction; SAXS, small-angle X-ray scattering; 2D-SAXS, two-dimensional SAXS; 1D-SAXS, one-dimensional SAXS; SIC, strain-induced crystallization

■ REFERENCES

(1) Mannsfeld, S. C.; Tee, B. C.; Stoltenberg, R. M.; Chen, C. V.; Barman, S.; Muir, B. V.; Sokolov, A. N.; Reese, C.; Bao, Z. Highly Sensitive Flexible Pressure Sensors with Microstructured Rubber Dielectric Layers. *Nat. Mater.* **2010**, *9*, 859−864.

(2) Chen, S.; Sun, L.; Zhou, X.; Guo, Y.; Song, J.; Qian, S.; Liu, Z.; Guan, Q.; Meade Jeffries, E.; Liu, W.; Wang, Y.; He, C.; You, Z. Mechanically and Biologically Skin-Like Elastomers for Bio-Integrated Electronics. *Nat. Commun.* **2020**, *11*, No. 1107.

(3) Shi, L.; Zhu, T.; Gao, G.; Zhang, X.; Wei, W.; Liu, W.; Ding, S. Highly Stretchable and Transparent Ionic Conducting Elastomers. *Nat. Commun.* **2018**, *9*, No. 2630.

(4) Zhang, W.; Wu, B.; Sun, S.; Wu, P. Skin-Like Mechanoresponsive Self-Healing Ionic Elastomer from Supramolecular Zwitterionic Network. *Nat. Commun.* **2021**, *12*, No. 4082.

(5) Markvicka, E. J.; Bartlett, M. D.; Huang, X.; Majidi, C. An Autonomously Electrically Self-Healing Liquid Metal-Elastomer Composite for Robust Soft-Matter Robotics and Electronics. *Nat. Mater.* **2018**, *17*, 618−624.

(6) Kaltenbrunner, M.; Sekitani, T.; Reeder, J.; Yokota, T.; Kuribara, K.; Tokuhara, T.; Drack, M.; Schwodiauer, R.; Graz, I.; Bauer-Gogonea, S.; Bauer, S.; Someya, T. An Ultra-Lightweight Design for Imperceptible Plastic Electronics. *Nature* **2013**, *499*, 458−463.

(7) Aubrey, M. L.; Axelson, J. C.; Engler, K. E.; Long, J. R. Dependence of Linker Length and Composition on Ionic Conductivity and Lithium Deposition in Single-Ion Conducting Network Polymers. *Macromolecules* **2021**, *54*, 7582−7589.

(8) Kang, J.; Son, D.; Wang, G. N.; Liu, Y.; Lopez, J.; Kim, Y.; Oh, J. Y.; Katsumata, T.; Mun, J.; Lee, Y.; Jin, L.; Tok, J. B.; Bao, Z. Tough and Water-Insensitive Self-Healing Elastomer for Robust Electronic Skin. *Adv. Mater.* **2018**, *30*, No. 1706846.

(9) Li, X.; He, L.; Li, Y.; Chao, M.; Li, M.; Wan, P.; Zhang, L. Healable, Degradable, and Conductive Mxene Nanocomposite Hydrogel for Multifunctional Epidermal Sensors. *ACS Nano* **2021**, *15*, 7765−7773.
(10) Liu, Y.; Pharr, M.; Salvatore, G. A. Lab-on-Skin: A Review of Flexible and Stretchable Electronics for Wearable Health Monitoring. *ACS Nano* **2017**, *11*, 9614−9635.
(11) Kang, J.; Tok, J. B. H.; Bao, Z. A. Self-Healing Soft Electronics. *Nat. Electron.* **2019**, *2*, 144−150.
(12) Zhang, Y.; Khanbareh, H.; Roscow, J.; Pan, M.; Bowen, C.; Wan, C. Y. Self-Healing of Materials under High Electrical Stress. *Matter* **2020**, *3*, 989−1008.
(13) Yan, X.; Liu, Z.; Zhang, Q.; Lopez, J.; Wang, H.; Wu, H. C.; Niu, S.; Yan, H.; Wang, S.; Lei, T.; Li, J.; Qi, D.; Huang, P.; Huang, J.; Zhang, Y.; Wang, Y.; Li, G.; Tok, J. B.; Chen, X.; Bao, Z. Quadruple H-Bonding Cross-Linked Supramolecular Polymeric Materials as Substrates for Stretchable, Antitearing, and Self-Healable Thin Film Electrodes. *J. Am. Chem. Soc.* **2018**, *140*, 5280−5289.
(14) Cao, Y.; Tan, Y. J.; Li, S.; Lee, W. W.; Guo, H. C.; Cai, Y. Q.; Wang, C.; Tee, B. C. K. Self-Healing Electronic Skins for Aquatic Environments. *Nat. Electron.* **2019**, *2*, 75−82.
(15) Annabi, N.; Shin, S. R.; Tamayol, A.; Miscuglio, M.; Bakooshli, M. A.; Assmann, A.; Mostafalu, P.; Sun, J. Y.; Mithieux, S.; Cheung, L.; Tang, X. S.; Weiss, A. S.; Khademhosseini, A. Highly Elastic and Conductive Human-Based Protein Hybrid Hydrogels. *Adv. Mater.* **2016**, *28*, 40−49.
(16) Guo, X. W.; Zhang, C. G.; Shi, L.; Zhang, Q.; Zhu, H. Highly Stretchable, Recyclable, Notch-Insensitive, and Conductive Polyacrylonitrile-Derived Organogel. *J. Mater. Chem. A* **2020**, *8*, 20346−20353.
(17) Kazem, N.; Bartlett, M. D.; Majidi, C. Extreme Toughening of Soft Materials with Liquid Metal. *Adv. Mater.* **2018**, *30*, No. 1706594.
(18) Xu, J. H.; Chen, P.; Wu, J. W.; Hu, P.; Fu, Y. S.; Jiang, W.; Fu, J. J. Notch-Insensitive, Ultrastretchable, Efficient Self-Healing Supramolecular Polymers Constructed from Multiphase Active Hydrogen Bonds for Electronic Applications. *Chem. Mater.* **2019**, *31*, 7951−7961.
(19) Tian, Y.; Wei, X.; Wang, Z. J.; Pan, P.; Li, F.; Ling, D.; Wu, Z. L.; Zheng, Q. A Facile Approach to Prepare Tough and Responsive Ultrathin Physical Hydrogel Films as Artificial Muscles. *ACS Appl. Mater. Interfaces* **2017**, *9*, 34349−34355.
(20) Cai, Y.; Shen, J.; Yang, C. W.; Wan, Y.; Tang, H. L.; Aljarb, A. A.; Chen, C.; Fu, J. H.; Wei, X.; Huang, K. W.; Han, Y.; Jonas, S. J.; Dong, X.; Tung, V. Mixed-Dimensional Mxene-Hydrogel Heterostructures for Electronic Skin Sensors with Ultrabroad Working Range. *Sci. Adv.* **2020**, *6*, No. eabb5367.
(21) Wang, X.; Zhan, S.; Lu, Z.; Li, J.; Yang, X.; Qiao, Y.; Men, Y.; Sun, J. Healable, Recyclable, and Mechanically Tough Polyurethane Elastomers with Exceptional Damage Tolerance. *Adv. Mater.* **2020**, *32*, No. 2005759.
(22) Sun, J. Y.; Zhao, X.; Illeperuma, W. R.; Chaudhuri, O.; Oh, K. H.; Mooney, D. J.; Vlassak, J. J.; Suo, Z. Highly Stretchable and Tough Hydrogels. *Nature* **2012**, *489*, 133−136.
(23) Li, Y. H.; Li, W. J.; Sun, A. L.; Jing, M. F.; Liu, X. J.; Wei, L. H.; Wu, K.; Fu, Q. A Self-Reinforcing and Self-Healing Elastomer with High Strength, Unprecedented Toughness and Room-Temperature Reparability. *Mater. Horiz.* **2021**, *8*, 267−275.
(24) Tan, Y. J.; Godaba, H.; Chen, G.; Tan, S. T. M.; Wan, G.; Li, G.; Lee, P. M.; Cai, Y.; Li, S.; Shepherd, R. F.; Ho, J. S.; Tee, B. C. K. A Transparent, Self-Healing and High-Kappa Dielectric for Low-Field-Emission Stretchable Optoelectronics. *Nat. Mater.* **2020**, *19*, 182−188.
(25) Vatankhah-Varnosfaderani, M.; Keith, A. N.; Cong, Y.; Liang, H.; Rosenthal, M.; Sztucki, M.; Clair, C.; Magonov, S.; Ivanov, D. A.; Dobrynin, A. V.; Sheiko, S. S. Chameleon-Like Elastomers with Molecularly Encoded Strain-Adaptive Stiffening and Coloration. *Science* **2018**, *359*, 1509−1513.
(26) Wang, Z.; Jiang, F.; Zhang, Y.; You, Y.; Wang, Z.; Guan, Z. Bioinspired Design of Nanostructured Elastomers with Cross-Linked Soft Matrix Grafting on the Oriented Rigid Nanofibers to Mimic Mechanical Properties of Human Skin. *ACS Nano* **2015**, *9*, 271−278.
(27) Yang, W.; Sherman, V. R.; Gludovatz, B.; Schaible, E.; Stewart, P.; Ritchie, R. O.; Meyers, M. A. On the Tear Resistance of Skin. *Nat. Commun.* **2015**, *6*, No. 6649.
(28) Wang, X.; Li, Y.; Qian, Y.; Qi, H.; Li, J.; Sun, J. Mechanically Robust Atomic Oxygen-Resistant Coatings Capable of Autonomously Healing Damage in Low Earth Orbit Space Environment. *Adv. Mater.* **2018**, *30*, No. 1803854.
(29) Wang, J.; Zhang, X.; Zhang, S.; Kang, J.; Guo, Z.; Feng, B.; Zhao, H.; Luo, Z.; Yu, J.; Song, W.; Wang, S. Semi-Convertible Hydrogel Enabled Photoresponsive Lubrication. *Matter* **2021**, *4*, 675−687.
(30) Greensmith, H. W. Rupture of Rubber. X., The Change in Stored Energy on Making a Small Cut in a Test Piece Held in Simple Extension. *J. Appl. Polym. Sci.* **1963**, *7*, 993−1002.
(31) Chang, G.; Yang, L.; Yang, J.; Stoykovich, M. P.; Deng, X.; Cui, J.; Wang, D. High-Performance Ph-Switchable Supramolecular Thermosets *Via* Cation-Pi Interactions. *Adv. Mater.* **2018**, *30*, No. 1704234.
(32) Gui, Q.; He, Y.; Wang, Y. Soft Electronics Based on Liquid Conductors. *Adv. Electron. Mater.* **2020**, *7*, No. 2000780.
(33) Wu, X.; Gao, N.; Jia, H.; Wang, Y. Thermoelectric Converters Based on Ionic Conductors. *Chem.—Asian J.* **2021**, *16*, 129−141.
(34) Higaki, Y.; Suzuki, K.; Ohta, N.; Takahara, A. Strain-Induced Molecular Aggregation States around a Crack Tip in a Segmented Polyurethane Film under Uniaxial Stretching. *Polymer* **2017**, *116*, 458−465.
(35) Song, Y.; Liu, Y.; Qi, T.; Li, G. L. Towards Dynamic but Supertough Healable Polymers through Biomimetic Hierarchical Hydrogen-Bonding Interactions. *Angew. Chem., Int. Ed.* **2018**, *57*, 13838−13842.
(36) Filippidi, E.; Cristiani, T. R.; Eisenbach, C. D.; Waite, J. H.; Israelachvili, J. N.; Ahn, B. K.; Valentine, M. T. Toughening Elastomers Using Mussel-Inspired Iron-Catechol Complexes. *Science* **2017**, *358*, 502−505.
(37) Song, P.; Xu, Z.; Dargusch, M. S.; Chen, Z. G.; Wang, H.; Guo, Q. Granular Nanostructure: A Facile Biomimetic Strategy for the Design of Supertough Polymeric Materials with High Ductility and Strength. *Adv. Mater.* **2017**, *29*, No. 1704661.
(38) Yoshida, S.; Ejima, H.; Yoshie, N. Tough Elastomers with Superior Self-Recoverability Induced by Bioinspired Multiphase Design. *Adv. Funct. Mater.* **2017**, *27*, No. 1701670.
(39) Zhao, X.; Chen, X.; Yuk, H.; Lin, S.; Liu, X.; Parada, G. Soft Materials by Design: Unconventional Polymer Networks Give Extreme Properties. *Chem. Rev.* **2021**, *121*, 4309−4372.
(40) Flory, P. J. Molecular Theory of Rubber Elasticity. *Polymer* **1979**, *20*, 1317−1320.
(41) Toki, S.; Sics, I.; Hsiao, B. S.; Tosaka, M.; Poompradub, S.; Ikeda, Y.; Kohjiya, S. Probing the Nature of Strain-Induced Crystallization in Polyisoprene Rubber by Combined Thermomechanical and in Situ X-Ray Diffraction Techniques. *Macromolecules* **2005**, *38*, 7064−7073.
(42) Lu, X.; Luo, Y.; Li, Y.; Bao, C.; Wang, X.; An, N.; Wang, G.; Sun, J. Polymeric Complex Nanoparticles Enable the Fabrication of Mechanically Superstrong and Recyclable Poly(Aryl Ether Sulfone)-Based Polymer Composites. *CCS Chem.* **2020**, *2*, 524−532.
(43) Das, S.; Martin, P.; Vasilyev, G.; Nandi, R.; Amdursky, N.; Zussman, E. Processable, Ion-Conducting Hydrogel for Flexible Electronic Devices with Self-Healing Capability. *Macromolecules* **2020**, *53*, 11130−11141.

https://doi.org/10.1021/acs.macromol.1c01976
Macromolecules 2021, 54, 10767−10775